Periodica Polytechnica
Chemical Engineering

61(2), pp. 133-143, 2017
https://doi.org/10.3311/PPch.9207

RESEARCH ARTICLE

Performance Evaluation of Hollow Fiber Membrane Contactors for Dispersion-Free Extraction of Cu^{2+} through Modelling and Simulation

Amir Muhammad[1], Wajid Ali[1], Iftikhar Ahmad[1], Mohammad Younas[1*]

Received 18 March 2016; accepted after revision 25 June 2016

Abstract

In this work extraction of copper (II) (Cu^{2+}) from aqueous solution has been studied theoretically in commercially available hollow fiber membrane contactors (HFMCs) X-40 and X-50 modules from Liqui Cel™. Trifluoro-acetylacetone (TFA) has been used as extractant. A mathematical model based on resistance-in-series has been presented to investigate the mass transfer mechanism and distribution of Cu^{2+} at interface. Model simulation was performed for various hydrodynamics and membrane geometrical characteristics in order to determine the solute efficiency, transmembrane flux and height of transfer unit (HTU) for both modules. In case of X-40 module, extraction efficiency reached to 78 % when the feed flowrate was 1.67 m^3s^{-1} while that for X-50, it was found to be just 20 % under same hydrodynamic conditions. On the basis of model results it was inferred that HFMCs could be the appropriate devices for extraction owing to exceptional low HTU value.

Keywords

Hollow Fiber Membrane Contactors, copper (II), dispersion free solvent extraction, trifluoro-acetylacetone

[1] Department of Chemical Engineering,
University of Engineering and Technology, Peshawar,
P.O. Box. 814, University Campus Peshawar 25120, Pakistan

[*] Corresponding author, e-mail: m.younas@uetpeshawar.edu.pk

1 Introduction

The development of efficient processes for extraction of valuable metals from industrial effluents have been the important subject in separation technology [1]. Concerns about saving natural resources and energy are increasing day by day. New techniques have been emerged to address these issues in particularly. Hollow fiber membrane contactor (HFMC) is one of the emerging separation technologies, which is in development stage for separation of both liquid and gas mixtures [2-4].

HFMCs as Cu^{2+} extraction devices have been received the most attention in recent decades because of their several advantages. These devices resemble to shell and tube heat exchanger configuration where a bundle of porous hollow fibers is installed inside a shell casing. Aqueous feed containing Cu^{2+} solute is allowed to flow in shell side while the organic extractant normally flows in tube side (inside the hollow fibers). Because of the hydrophobic nature of extractant it penetrates into the pores of membrane and comes into contact with Cu^{2+} at the membrane-feed interface. Cu^{2+} then reacts with organic extractant and the resultant complex is transferred to shell from tube-membrane interface due to the concentration gradient. Because of the non-dispersive contact between feed and extractant, HFMCs offer a number of advantages over conventional extractors (column contactors). These include independent feed and extractant flow rates with no flooding, entraining and channelling, higher mass transfer interfacial area, no or less extractant loss, easy and straightforward scale-up because of invariable contact area [4, 5]. However, despite its great prospective, the membrane contactors are still seeking their use in industrial processes. Substantial efforts are required for process modelling, right choice of membrane and well-chosen optimal operating parameters in order to employ membrane contactors commercially for Cu^{2+} extraction [6].

Mass transfer modelling of HFMCs is inevitable to study the concentration and flux profiles, to investigate the solute transport, to categorise the controlling resistance and for the optimisation of the process operating parameters. Recently mass transfer modelling of HFMCs have caught the attention of several researchers. For example, Gonzglez-Mufioz et al. [7]

developed a resistance-in-series mass transfer mathematical model for simulation of integrated extraction and stripping process in HFMCs. The model was used for the prediction of unsteady-state concentration profiles of both aqueous feed and extractant phase in a single process. Juang et al. [8] studied the extraction of Cu^{2+} in a HFMC both experimentally and theoretically. The mass transfer mathematical model they developed was based on resistances in series approach. Model was used to compare the relative resistance of each diffusion step i-e aqueous phase, membrane and organic phase and it was found that all these played a major role for the recovery of copper. A resistance in series model was also presented by Bocquet et al. [9] to study the dispersion free extraction of aroma compounds in HFMC X-30 and X-40 modules. The validity of model was tested for the extraction of four different aroma solutes. Model was simulated to predict the effects of membrane characteristics and process parameters on extraction efficiency. This model was later modified by Younas et al. [5] for the recovery of Cu^{2+} from aqueous feed with different solvents using HFMCs. The model findings of aforementioned scientists fitted very well with experimental results. Recently some CFD models have also been proposed that are based on mass and momentum balance conservation equations.

Although several mass transport models have been developed by different researchers however, limited work is available about the mass transfer mechanism and characterisation of HFMCs [10, 11]. Previous studies [5, 27] have focused mainly on the transport of solute across HFMCs and the resistances that hinder this transport. Scale up of HFMCs has not been widely studied for liquid-liquid extraction in existing literature. More theoretical investigation is required to encourage the entrepreneurs to utilize HFMCs for the selected application at large scale.

In the current work, mass transfer analysis of two different modules of HFMC has been described. Performance analysis has been discussed for HFMC modules X-40 (baffled) and X-50 (baffle less), fabricated by Liqui-Cel™, for the extraction of Cu^{2+} from aqueous solution with TFA diluted in 1-decanol at 25 °C as a base case simulation. Resistance-in-series approach was adopted on membrane and its boundary layers to develop mathematical model. Simulation has been performed to investigate the effects of membrane structural characteristics, hydrodynamics and the module geometry for extraction efficiency and solute mass flux. The current work provides an insight into the phenomenon and its implications in scale-up of a membrane based liquid-liquid extraction system.

2 Studied System

This study is focused on the modelling of once through HFMC based extraction system. The steady state model thus developed is able to predict the solute concentration at the exit of module as a function of desired operating conditions. The schematic representation of pilot plant is shown in Fig. 1. Aqueous solution of Cu^{2+} is passed through shell of the module and the organic phase which was a mixture of 15 % v/v TFA in n-decanol was passed inside the fibers. As described in previous studies [5, 27] such flow configuration results in higher extraction efficiency. Allowing the aqueous phase to flow in shell side of module increases the surface area as compared to inside fibers. The overall mass transfer coefficient has also been found to increase which causes a faster extraction of solute.

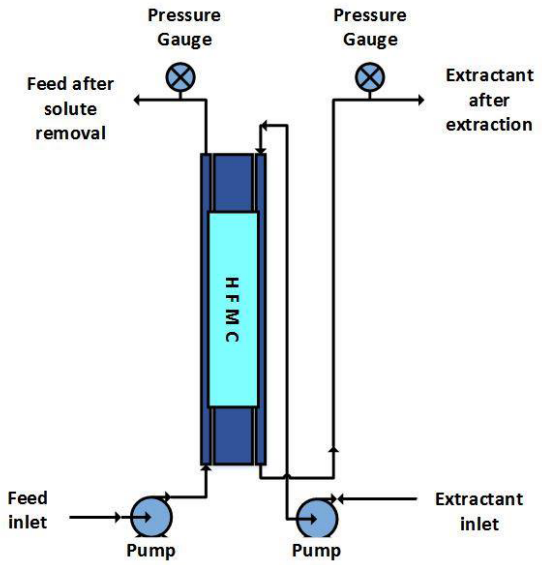

Fig. 1 HFMC based once through extraction

A slightly higher pressure was applied on tube side in order to immoblize the organic phase in the pores mouth at tube-membrane interface and to avoid its dispersion in aquesous feed. When the two phases come into contact at immobilzed interface, Cu^{2+} reacts with extractant to form copper-complex and consequently transfers from feed solution to the extractant because of the concentration gradient. Simulation considered the plant to be operated in such a way that each time fresh feed and extractant make contact in module. Two different HFMC modules X-40 (baffled) and X-50 (baffle less) fabricated by Liqui-Cel™ have been used in dispersion-free extraction of Cu^{2+}. The geometical characterictics of both modules are shown in Table 1.

3 Theory

In HFMCs the dispersion free extraction of solute takes place through a combined phenomenon of convection and diffusion. In this type of extraction, the function of membrane is to provide the surface and make a contact between the aqueous and organics phases. The driving force is the concentration gradient which is responsible for the mass transfer between the two phases across the membrane [4]. It is desired to maximize mass transfer by optimizing the design and process parameters. The diffusion flux model equation is given by [12]

$$J_i = k_i \left(C_i - C_i^* \right) \tag{1}$$

Table 1 HFMC module characteristics provided by the manufacturer or taken from literature [5, 27]

Geometrical characteristics	Liqui-Cel™ Module X-40	Liqui-Cel™ Module X-50
Internal diameter of the fiber (m)	2×10^{-4}	2.2×10^{-4}
External diameter of the fiber (m)	3×10^{-4}	3×10^{-4}
Mean diameter of pore (m)	3×10^{-8}	4×10^{-8}
Diameter of the module shell (m)	4.90×10^{-2}	4.25×10^{-2}
Length of the module (m)	146.2×10^{-3}	121.8×10^{-3}
Number of fibers [-]	10000	7400
Porosity (%)	25	40
Aqueous side diffusion coefficient (m^2s^{-1})	2.79×10^{-9}	
Organic side diffusion coefficient (m^2s^{-1})	$1.31\times10^{-10}m^2/s$	

Where J stands for the solute flux of solute i, k for mass transfer coefficient and C denotes the concentration of the solute. C^* is concentration at interface. Likewise convective flux model equation is given by [13]

$$J_i = A_i q_i \left(C_i^{in} - C_i\right) \tag{2}$$

Here A is the mass transfer interfacial area between the two phases. "q" represents the flowrate of the individual phase flowing in the module. The theoretical mass transfer analysis incorporates mass balances of solute and extractant and the partitioning equilibrium of solute-solvent extraction system. The extent of solute transferred across the membrane is controlled by partition coefficient denoted here by P. It is defined as the ratio of Cu^{2+} concentration in organic phase to that in the aqueous phase at equilibrium and is given as [14]

$$P = \frac{C_{i\,sol}}{C_{iaq}^*} \tag{3}$$

For modelling purpose the mass transfer correlations are indispensable. Several authors have made greater contribution for the estimation of various correlations and are available in the literature [4, 15, 16]. The mass transfer correlation shown by Eq. (4) an (5) have been used for the fluid flowing in shell side of the module X-40 and X-50, respectively [17, 18].

$$Sh = 0.32\,\mathrm{Re}^{0.61}\,Sc^{0.33} \tag{4}$$

$$Sh = 8.71\left(d_h \big/ L\right)\mathrm{Re}^{0.74}\,Sc^{0.33} \tag{5}$$

Sh, Re, Sc are the dimensionless numbers termed as Sherwood number, Reynolds number and Schmidt number, respectively, used to find the correlations of mass transfer coefficient. d_h and L denote hydraulic diameter and length of module respectively. Mass transfer coefficient in the pores of the membrane depends upon the structural characteristics of the membrane and solute diffusion coefficient. As the membrane used is hydrophobic, therefore organic phase fills in membrane's pores. Membrane side mass transfer coefficient based on organic phase is given by [19]

$$k_{mb} = \frac{D_{org}\varepsilon}{\sigma\tau} \tag{6}$$

Where D_{org} is the diffusion coefficient of copper complex in organic phase, σ is the thickness of the membrane, ε and τ are the porosity and tortuosity of the membrane respectively. Wakao-Smith [20, 21] gave the following relation between ε & τ.

$$\tau = \frac{1}{\varepsilon} \tag{7}$$

Likewise mass transfer correlations for fluid flowing inside lumen of both the modules is described by Leveque equation and widely applied by various researchers using solute extraction in the same modules [22-24].

$$\begin{aligned} Sh &= 1.62Gz^{0.33} \quad \text{for } Gz > 6 \\ Sh &= 0.5Gz \qquad\;\; \text{for } Gz \le 6 \end{aligned} \tag{8}$$

$$k = \frac{S_h D}{d_{\mathrm{int}}} \tag{9}$$

Here Gz stands for dimensionless Graetz number. Overall mass transfer coefficient, denoted by K, for aqueous phase flowing through shell side is calculated based on resistances-in-series model and it was found to be [25, 26]

$$\frac{1}{K_{aq}} = \frac{1}{k_{aq}} + \frac{d_{ext}}{Dk_{mb}d_{lm}} + \frac{d_{ext}}{Dk_{org}d_{\mathrm{int}}} \tag{10}$$

For organic phase flowing in shell, above equation becomes

$$\frac{1}{K_{aq}} = \frac{1}{k_{aq}} + \frac{d_{\mathrm{int}}}{Dk_{mb}d_{lm}} + \frac{d_{\mathrm{int}}}{Dk_{org}d_{ext}} \tag{11}$$

Partition coefficient is a limiting parameter which defines the extent of extraction. Maximum possible extraction based on the partition coefficient is denoted by "ϕ" and is given by [27]

$$\phi = 1 - \frac{C_{out}}{C_{in}} \tag{12}$$

The key indicator to evaluate the performance of HFMC to obtain the desired solute extraction in once-through mode is the height of a transfer unit (HTU), which also reflects the efficiency of the module. It is given by [28]

$$HTU = \frac{q_{aq}}{K_{aq} a A} \tag{13}$$

where a is the interfacial area per unit volume. On the other hand, the number of transfer units (NTU) is a measure of the difficulty of the separation. NTU is defined as change in concentration of fluid for the unit driving force responsible for the transfer of solute. In current research work driving force is the concentration gradient of Cu^{2+} between the two phases being contacted [29].

$$NTU = \int_{C^{in}}^{C^{out}} \frac{dC}{C - C^*} \tag{14}$$

Theoretical length of the module, denoted by Z, is suggested which meets the desired extraction under the specified conditions of solute, solvent and operating parameters [30].

$$Z = HTU \times NTU \tag{15}$$

For simplicity, the modules are assumed to compose of flow-cells. A flow-cell is defined as tubular extractor which encapsulates the single fiber. Thus the whole hollow fiber membrane contactor module is divided into equal number of flow-cells which means that the total flow-cells and fibers are equal in the module [31].

4 Methodology

The module length, diameter and packing density are the key design parameters to be calculated to obtain the desired solute extraction under the specified operating conditions. Experiments were performed for once-through mode i-e without recirculation of both the phases in HFMC modules of X-40 and X-50. Initial concentration of Cu^{2+} was taken as 7.8 $molm^{-3}$. The TFA was taken 15 % v/v diluted in 1-decanol equivalent to 1798 $molm^{-3}$. The experiments were performed at 25±2 °C. Partition coefficient for this extraction system was measured to be 6.9 [27]. The flowrate of the aqueous phase was varied for each experiment while other parameters were kept constant. Aqueous solution was allowed to flow in the shell of the module and counter-current to organic phase flowing inside fibers.

Simulation was run to study the influence of hydrodynamics and structural parameters of the module on extraction efficiency, Cu^{2+} flux, HTU and theoretical length of the module in order to achieve the desired extraction. The coupled model was validated for extraction efficiency against various values of feed flow rate in both the modules.

5 Results and discussions

5.1 Effect of hydrodynamics on module performance

Simulation was run to find the effect of feed and organic phase hydrodynamics on extraction efficiency and flux. Initial copper concentration in feed was 7.8 $molm^{-3}$ while that of TFA in solvent was 1798 $molm^{-3}$. Aqueous phase flow rates were chosen within the range of 1.67×10^{-6} to 1.67×10^{-5} m^3s^{-1}. The organic phase flow rate was held constant at 5×10^{-6} m^3s^{-1}. Simulation has been performed for both X-40 & X-50 modules. The results are plotted for extraction efficiency and flux against feed flow rate on x-axis. From the Fig. 2 it can be observed that for both the modules, flux increases with increasing aqueous phase flow rate. Furthermore, X-40 module guarantees higher flux than achieved by X-50 under same operating conditions. The higher flux obtained by X-40 module is due to larger interfacial area for the solute contact with the organic solvent (1.3 m^2 & 0.85 m^2 for X-40 & X-50 respectively).

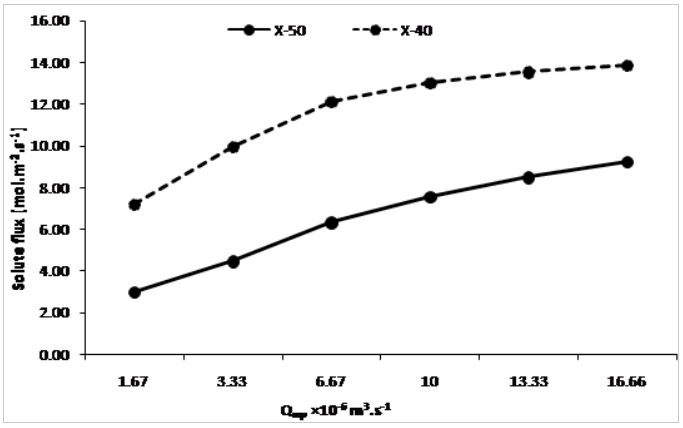

Fig. 2 Effect of feed flowrate on Cu^{2+} flux, $Q_{org} = 5\times10^{-6}$ m^3s^{-1}. Counter flow: $C_{ini}^{Cu2+} = 7.8molm^{-3}$, $C_{ini}^{TFA} = 1798molm^{-3}$, P = 6.9, T = 25±2 °C

In contrast to the above pattern, Fig. 3 represents that higher efficiency can be obtained at lower flowrate of aqueous phase for both modules. However performance of X-40 is found to be approximately 4 times much better than that of X-50 module. Maximum extraction efficiency of former one ranges up to 78% while that of later one is 20% at the minimum aqueous flow rate. The plausible justification for reduced efficiency at the higher flow rate could be that solute finds lesser contact time with solvent, thus causing reduction in extraction efficiency.

Higher efficiency offered by X-40 module could be due to the presence of baffle in it, which are responsible for promoting the turbulence that in turn lead to better performance.

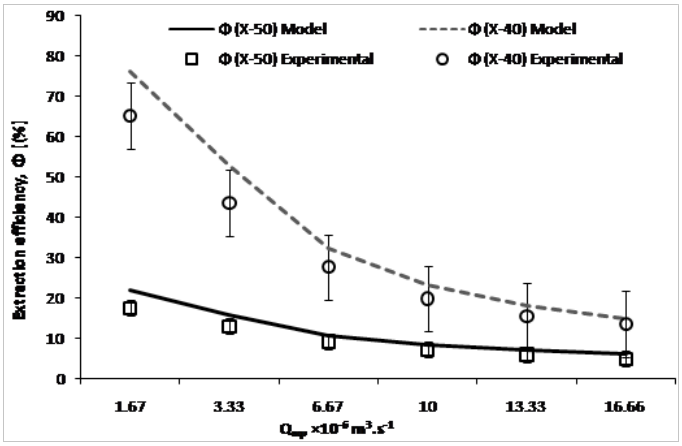

Fig. 3 Effect of feed flow rate on extraction efficiency, $Q_{org} = 5\times10^{-6}\ m^3s^{-1}$ Counter flow, $C_{ini}^{Cu2+} = 7.8molm^{-3}$, $C_{ini}^{TFA} = 1798molm^{-3}$, P = 6.9, T = 25±2 °C

5.2 Effect of hydrodynamics on HTU

As it has been discussed earlier that HTU is the height of transfer unit and reflects the efficiency of the column. Small values of HTU designate the lower theoretical height of the column to achieve the desired mass transfer, meaning the efficient and fast extraction. This provides the better design of membrane contactors to accomplish the maximum possible extraction. In the literature, HTU is sometimes used to designate the length of contacting device since the membrane contactor may not necessarily orient vertically. By observing the Fig. 4 we can sensibly conclude that HTU offered by X-40 module is much lower than that of X-50 module for both flow configurations. Least value of HTU is offered by X-40 module when aqueous feed is in shell side; this confirms our previous results that better efficiency is offered by X-40 module.

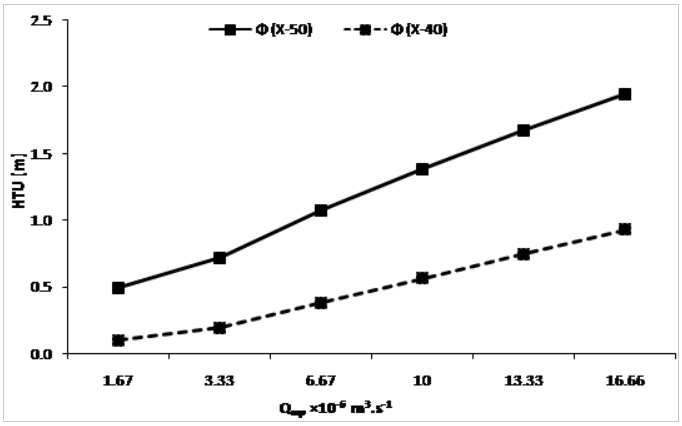

Fig. 4 Effect of feed flow rate on HTU, $Q_{org} = 5\times10^{-6}\ m^3s^{-1}$. Counter flow, $C_{ini}^{Cu2+} = 7.8molm^{-3}$, $C_{ini}^{TFA} = 1798molm^{-3}$, P= 6.9, T = 25±2 °C

Figure 4 shows that X-50 module with aqueous phase in shell side gives highest HTU as compared to that for X-40, indicating that the poorest performance is exhibited by this combination. Highest efficiency as indicated by least HTU for X-40 module is in fact due to higher mass transfer coefficient and higher interfacial area which is also clear from Eq. (13). The least HTU value of 10 cm was obtained which is in closest agreement with the literature values reported by Prasad and Sirkar [32]. On the other hand, if organic flow is introduced in shell side of X-50, HTU value further increases which consequently reduces further the module efficiency. Thus when comparing the flow configurations it can easily be abstracted that for both the modules, HTU is low when aqueous phase is routed through the shell side of the membrane. In fact shell side of the module offered larger surface area than tube side thus lowering the HTU value which ultimately is responsible for better extraction efficiency.

5.3 Effect of module geometry on module performance

The design of a membrane contactor module means to define the geometry of the module. An efficient membrane contactor is capable to extract the desired solute from the solution. Solute extraction is not only affected by the contact time between the solute and solvent but module structure also plays an important role in effective extraction. By the structure of module we mean to specify its diameter and length in order to achieve the desired level of extraction. Also, an efficient and a good design of membrane contactor requires choosing the precise values of packing density, porosity, diameter and thickness of the membrane.

The simulation was run to study the influence of structural parameters of the membrane and the module. The flow rates were kept constant in both sides of the membrane at $5\times10^{-6}\ m^3s^{-1}$ in both the modules for once through extraction of Cu^{2+}. Interest has been taken to study the solute extraction efficiency of the module, solute flux through the membrane, height of transfer unit (HTU) and number of transfer unit (NTU).

5.3.1 Effect of packing fraction

Extraction efficiency and flux was plotted versus packing fraction as shown in Fig. 5. Packing fraction, denoted by P_f, of a module is defined from the following relationship,

$$P_f = N \times \left(d_{ext} / d_s \right)^2 \tag{16}$$

Where N stands for the number of fibers inside the module and d_{ext} and d_s show the external diameter of fiber and diameter of the module shell, respectively.

The number of fibres are varied in order to measure the different values of packing fraction while the diameter of the fiber and shell was kept constant. Simulation was performed for the different values of packing fraction as determined in Table 2.

It is found from Fig. 5 that an increase in packing fraction increases the extraction efficiency. Packing fraction varies with number of fibers without changing the size of the module. However, increased packing fraction hinders the flow of solute across the membrane and flux is reduced. The results showed that effect in former are usually suppressed by the later one. Thus flux falls with the increase in packing fraction. Also by comparing the efficiency of the two different modules

i.e. X-50 and X-40 one can observe that extraction efficiency of X-40 module is more than that of X-50 module. The mass transfer coefficient and hence the efficiency enhances with the increase in packing fraction. This could be due to the fact that more area becomes available for solute transfer. Maximum efficiency attained for the packing fraction of 65-70%. The later decline is due to the formation of "dead zones". These are the regions where the fibers are close enough to each other, this obstructs the flow leading to the reduced efficiency [33].

Table 2 Packing fraction calculations

Number of fibers, N		Packing fraction (P_f)
X-50 Module $d_{ext} = 3\times10^{-4}$ m $d_s = 42.5\times10^{-3}$ m	X-40 Module $d_{ext} = 3\times10^{-4}$ m $d_s = 49\times10^{-3}$ m	$P_f = N\times\left(d_{ext}/d_s\right)^2$
2000	2660	0.10
5000	6645	0.25
7400	9836	0.37
10000	13294	0.50
13000	17282	0.65
15000	19939	0.75

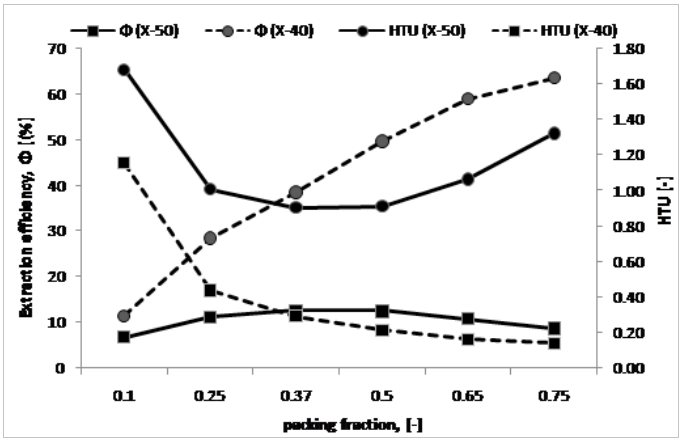

Fig. 5 Effect of packing fraction on extraction efficiency at $Q_{aq}=Q_{org}= 5\times10^{-6}$ m^{3}s^{-1}, counter flow, $C_{ini}^{Cu2+} = 7.8$molm^{-3}, $C_{ini}^{TFA} = 1798$molm^{-3}, P= 6.9, T = 25±2 °C

Figure 5 also describes the variation of HTU with the packing fraction. It has been discussed earlier that HTU reflects the efficiency of the column. By observing the above figure, we can judiciously conclude that HTU of X-40 module is much lower than that of X-50 module. This confirms our results that better efficiency is offered by X-40 module.

On the other hand when a wise comparison is made between the flow configurations it can easily be deducted that for both the modules, HTU is low when aqueous phase is routed through the shell side of the membrane. Interestingly, the enhanced efficiency of membrane contactor is not only due to the higher mass transfer coefficient. In fact mass transfer coefficient obtained with membrane contactors are usually same or even lower than those obtained with conventional column extractors. The increased efficiency is actually the consequence of increased interfacial area which is unchangeable with the operating conditions. Membrane contactors offer an area of 500 times more than what is obtainable in conventional dispersive contactors [34].

It is presented in Fig. 6 that the packing fraction has an inverse relation with the solute flux which is more effective in X-40 modules as compared to X-50. The least flux of 2 molm^{2}s^{-1} was reported in X-40 module at packing fraction of 0.75 while 9.1 molm^{2}s^{-1} was reported in X-50 modules at the same value of packing fraction. As we are increasing the number of fibers, packing fraction increases as a result the solute flux across the module decreases which results in increase of efficiency.

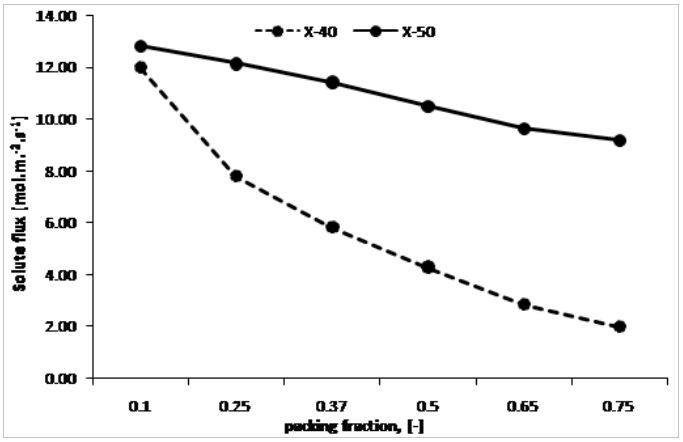

Fig. 6 Effect of module packing fraction on flux at $Q_{aq}=Q_{org}= 5\times10^{-6}$ m^{3}s^{-1}, counter flow, $C_{ini}^{Cu2+} = 7.8$molm^{-3}, $C_{ini}^{TFA} = 1798$molm^{-3}, P= 6.9, T = 25±2 °C

5.3.2 Effect of membrane thickness

Fibers thicken when their internal or external diameters increase. Simulation has been carried out to investigate the effect of thickness of the fiber ranging from 1×10^{-5} to 10×10^{-5}m. The corresponding values of external diameter were 2.4×10^{-5} to 4.2×10^{-5}m. Aqueous and organic flow rates were set at 5.0×10^{-6} m^{3}s^{-1}. Figure 7 compares the extraction efficiency of X-40 baffled and X-50 baffle less modules with respect to membrane fiber thickness. A decrease in extraction efficiency occurs with the increase in thickness of the fiber. This is due to the difficulty of the passage with the increased thickness across which solute has to travel. In other words mass transfer resistance offered by membrane rises with thickness leading to the lower flux and efficiency. If internal diameter is increased keeping the external one constant, this also leads to increase in fiber thickness, thus ultimately producing the same results. Additionally, if both the internal and external diameters increase in such a way as to keep the thickness constant, improved efficiency has been observed due to the availability of larger surface area.

As observed from Fig. 7 the HTU for both the modules tends to increase with the increase of fiber thickness up to 6×10^{-5} m but as we further increase fiber thickness, HTU starts to decrease

gradually and at higher values there is negligible effect on HTU. Similarly, by comparing the value of HTU we can see that there is considerable difference between HTU based on X-40 module and those based on X-50 module. The HTU for X-50 module are 2 to 5 times greater than those obtained by X-40 under the same working conditions. This is an indication of better performance offered by X-40 module. Surprisingly X-40 module presents same HTU at higher thickness with both flow configurations. In contrast the HTU based on X-50 module changed substantially when the flow configuration is changed.

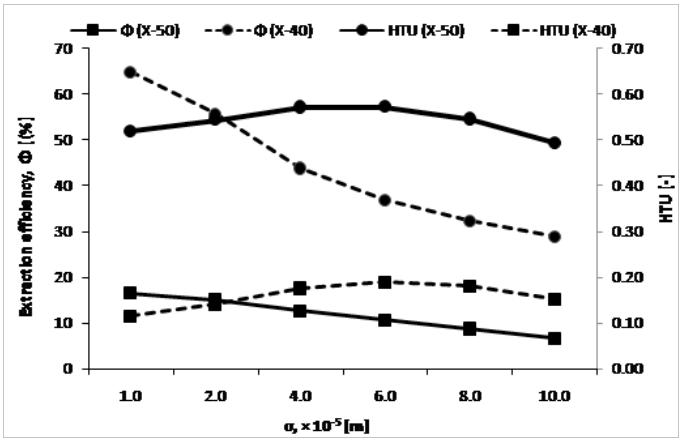

Fig. 7 Effect of fiber thickness on extraction efficiency and HTU at Q_{aq} = Q_{org} = 5×10^{-6} m^3s^{-1}, counter flow, C_{ini}^{Cu2+} = 7.8molm^{-3}, C_{ini}^{TFA} = 1798molm^{-3}, P= 6.9, T = 25±2 °C

It is shown in Fig. 8 that membrane thickness has an inverse relation with the solute flux for both X-40 and X-50 modules. The effect of fiber thickness on solute flux is quite significant at lower values which decrease gradually with the increase in thickness thus resulting in lower extraction efficiency. At higher values of thickness, it is difficult for the solute to pass through the membrane which results in a decrease of flux and hence affecting module performance. It can also be concluded that X-40 module has higher solute flux than X-50 which again supports our previous results which states that X-40 has better performance than X-50.

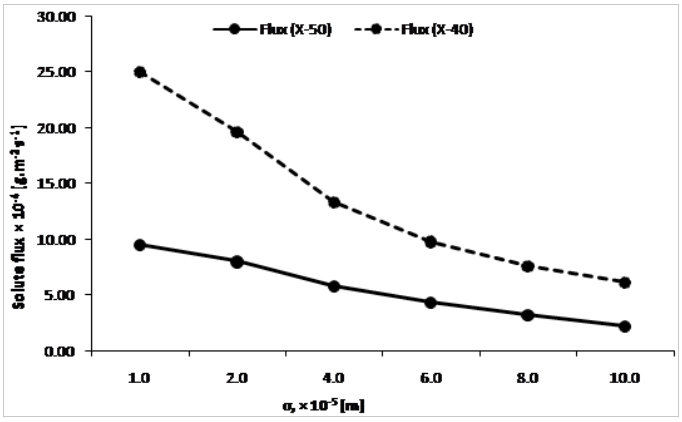

Fig. 8 Effect of fiber thickness on solute flux, Q_{aq} = Q_{org} = 5×10^{-6} m^3s^{-1}, counter flow, C_{ini}^{Cu2+} = 7.8molm^{-3}, C_{ini}^{TFA} = 1798molm^{-3}, P= 6.9, T = 25±2 °C

5.3.3 Effect of porosity to tortuosity ratio

Simulation was carried out to explore the effect of ε/τ ratio ranging from 0.02 to 0.64, which corresponds to the porosity of 20% to 80%. Fig. 9 shows these effects. It can be observed that with the rise in porosity to tortuosity ratio extraction efficiency enhances. Actually as this ratio increases more solute transfers across the membrane due to the increase in pore volume, leading to higher efficiency. Additionally extraction efficiency for the X-40 is greater than for the baffle-less X-50 module. Porosity to tortuosity ratio influences the membrane side mass transfer coefficient according to Eq. (7) and thus higher flux and enhanced extraction can be achieved by increasing this ratio [9].

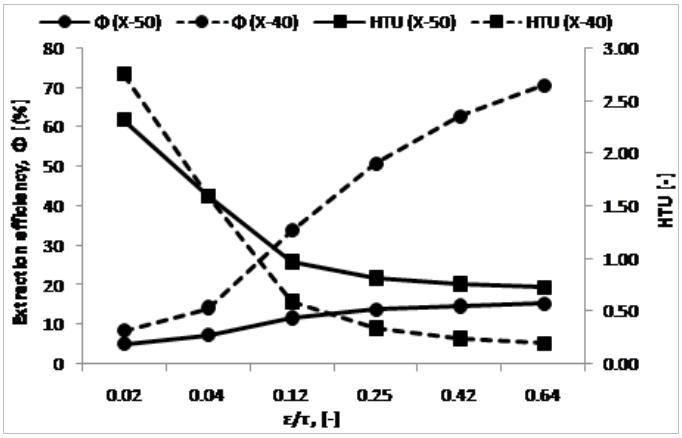

Fig. 9 Effect of porosity/ tortuosity ratio on efficiency and flux, Q_{aq} = Q_{org} = 5×10^{-6} m^3s^{-1}, counter-current flow, C_{ini}^{Cu2+} = 7.8molm^{-3}, C_{ini}^{TFA} = 1798molm^{-3}, P= 6.9, T = 25±2 °C

By comparing the value of HTU one can deduce that X-40 module with the aqueous phase flow through shell side has been proven to be most efficient, having the least value of HTU. Surprisingly, X-40 module with the organic phase flowing through shell side showed approximately the same value. In contrast, HTU for X-50 module are substantially higher indicating poor performance as compared to X-40 module. While analyzing the flow configuration, it is clear that X-40 module with the aqueous phase flow through shell side exhibits lower HTU value, enhanced performance as compared to that of X-50 module with the organic phase flow through shell side.

It is also presented in Fig. 10 that solute flux has a direct relation with (ε/τ) keeping other parameters constant. At low value of (ε/τ), there is no significant difference in flux for both X-40 and X-50 modules but as (ε/τ) increases to higher values, the effect on solute flux across the membrane becomes too large and it increases quite randomly. The maximum solute flux of 21×10^{-4} is reported for X-40 module at (ε/τ) value of 0.64 while keeping flow rates of both feed and organic phase constant. It is 4 times more than the flux of X-50 module at the same (ε/τ) value which is due to larger interfacial area and ultimately more contacts time of feed stream with the membrane.

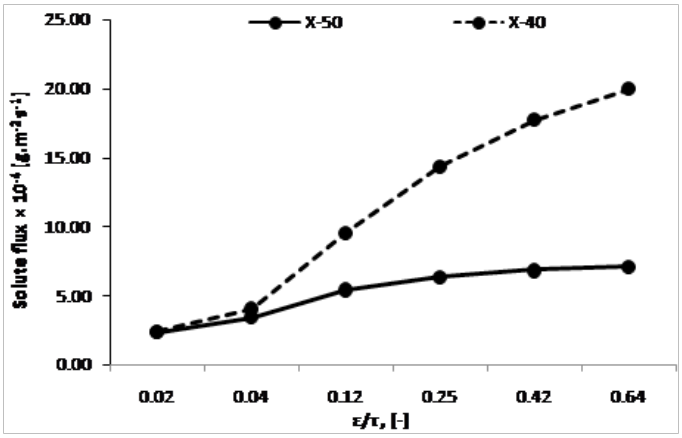

Fig. 10 Effect of porosity/tortuosity on solute flux, $Q_{aq}=Q_{org}= 5\times10^{-6}$ m^{3}s^{-1}, counter-current flow, $C_{ini}^{Cu2+} = 7.8$molm^{-3}, $C_{ini}^{TFA} = 1798$molm^{-3}, P= 6.9, T = 25±2 °C.

Both the modules studied here use membrane which is made of polypropylene. Although made of the same material, morphological and geometrical characteristics of membranes differ, for example X-40 membrane has a porosity of 0.25 and that of X-50 is 0.40 [5,27] and is enlisted in Table 1.

As shown by Eq. (6), the change in values of porosity/tortuosity changes the mass transfer coefficient within membrane. Flux is calculated by resistance in series model described in previous studies [5, 8, 27] in detail which is based on individual mass transfer coefficients in boundary layers on aqueous phase and organic phase sides and within membrane. It is worth noting that the correlation for mass transfer coefficient on aqueous side is different for both the modules e.g. X-40 and X-50 as described by Eq. (4) and (5), respectively. Change in values of ratio of porosity to tortuosity affects the flux for both the modules however, the quantitative effect is different due to their different correlations for Sherwood number. For low values of ratio of porosity to tortuosity the difference is not marginal on flux however, the effect becomes significant for flux in both modules due to the share of mass transfer coefficient within membrane. This is also important to note that mass transfer resistance within membrane decreases with the increase of porosity/tortuosity for both the modules however this effect is not same. Therefore effect of porosity/tortuosity on flux also differs in both modules.

5.3.4 Theoretical length of the module

The module length has been calculated from HTU and NTU by using Eq. (15) while keeping other parameters constant. It has been shown that increase in fiber length directly affects module length and a significant increase resulted in theoretical length of both X-40 and X-50 module for the organic phase in shell side.

Moreover, the extraction improves with length of the fibre due to high residence time and increase in interfacial area [5]. This results in better performance of membrane contactor but with reduced flux which is overcome by the other aforementioned factors.

The effective length of membrane module has an inverse relation with "ε/τ" ratio in any case whether feed is in the shell side or in the fiber. Simulation has been performed to explore the effect of ε/τ ratio from 0.02 to 0.64, which corresponds to the porosity of 20% to 80%. It can be concluded from Fig. 11 that at low value of "ε/τ" the effective length of membrane module is high while there is a rapid decrease in it with the increase in ε/τ up to a certain limit after which there is no effect of "ε/τ" on module length. The module length for X-50 is lesser than X-40 at lower "ε/τ" value while at higher value, the module length for X-50 is lower than X-40. It is also concluded that the module length is high for a given value of ε/τ when the organic phase is allowed to flow in shell side [35].

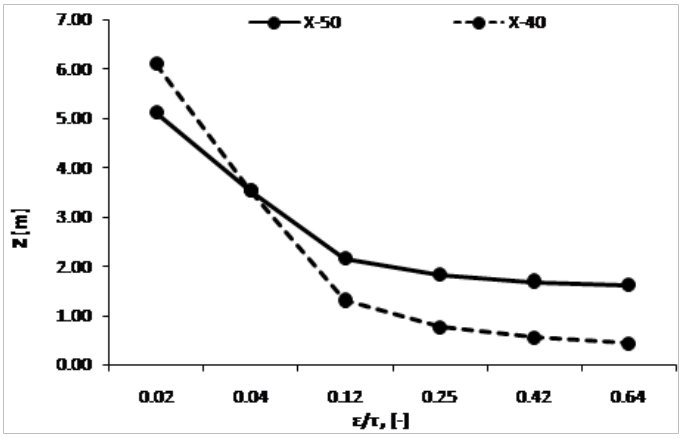

Fig. 11 Effect of porosity to tortuosity ratio on theoretical length, $Q_{aq}= Q_{org}= 5\times10^{-6}$ m^3.s^{-1}, counter flow, $C_{ini}^{Cu2+} = 7.8$molm^{-3}, $C_{ini}^{TFA} = 1798$molm^{-3}, P= 6.9, T = 25±2 °C

The effect of aqueous feed flow rate on theoritical length of module has been shown in Fig. 12. The increase in flow rate results in increase of flux and HTU due to which it has direct affect on the module length. But the extraction efficiency decreases drastically due to less residence/contact time for mass transfer (extraction of Cu^{2+} by TFA) and maximum pressure drop occurs at high flow rates.

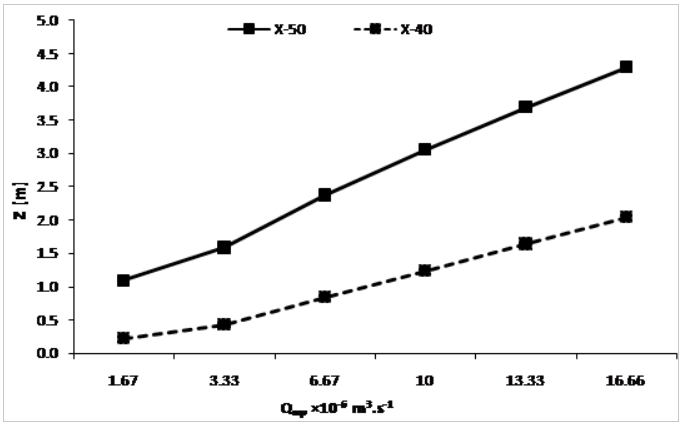

Fig. 12 Effect of feed flow rate on theoretical length, $Q_{aq}= Q_{org}= 5\times10^{-6}$ m^{3}s^{-1}, counter flow, $C_{ini}^{Cu2+} = 7.8$molm^{-3}, $C_{ini}^{TFA} = 1798$molm^{-3}, P= 6.9, T = 25±2 °C

It is found from Fig. 13 that an increase in packing fraction decreases module length and ultimately increases extraction efficiency. Packing fraction varies with number of fibers without changing the size of the module which promises for larger surface area and thus caused much solute to be extracted. On the other hand, increased packing density hinders the flow of solute through the membrane and thus flux is decreased.

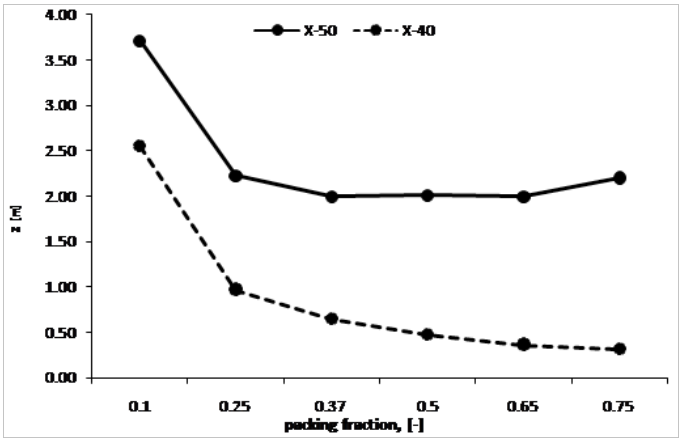

Fig. 13 Effect of module packing fraction on theoretical length, $Q_{aq} = Q_{org} = 5\times10^{-6}$ m^3.s^{-1}, counter flow, $C_{ini}^{Cu2+} = 7.8$molm^{-3}, $C_{ini}^{TFA} = 1798$molm^{-3}, P= 6.9, T = 25±2 °C.

There is also a significant effect of membrane thickness on module length for both X-40 baffled and X-50 baffle less modules. Figure 14 shows that module length for X-50 module is 2 to 4 times greater than those obtained by X-40 with the same membrane thickness and under the same operating condition.

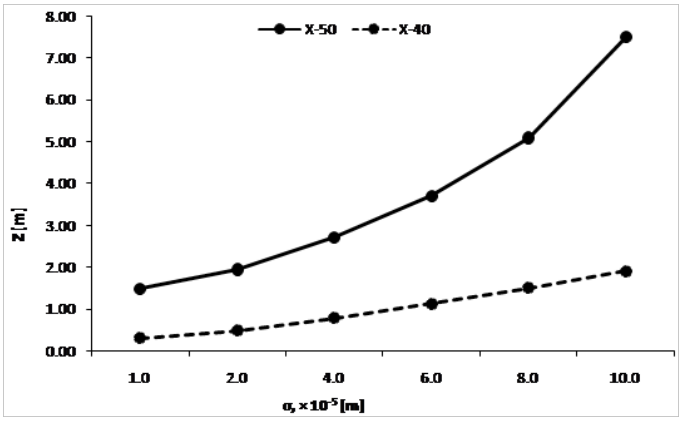

Fig. 14 Effect of membrane thickness on theoretical length, $Q_{aq} = Q_{org} = 5\times10^{-6}$ m^3.s^{-1}, counter flow, $C_{ini}^{Cu2+} = 7.8$molm^{-3}, $C_{ini}^{TFA} = 1798$molm^{-3}, P= 6.9, T = 25±2 °C

This is an indication of better performance offered by X-40 module. Surprisingly X-40 module presents same length at higher thickness with both flow configurations. In contrast, the module length based on X-50 module changed substantially when the flow configuration is changed.

6 Conclusions

Two different modules of HFMC, baffled X-40 and baffle less X-50 were used for the removal of Cu^{2+} from aqueous feed with an organic solvent TFA. Both the modules were simulated in MATLAB® 8.1.2 by varying the design and operating parameters to assess the efficiency and performance for the extraction of Cu^{2+}. Aqueous and organic phase were allowed to flow in tube and shell side of the membrane. It was concluded that when the organic phase flows in the tube side, X-40 modules has low porosity to tortuosity ratio, HTU and small module length which results in maximum flux and higher efficiency. Similarly, X-40 baffled module has 4-5 times higher flux than X-50 owing to larger contact area and higher number of fibres.

X-40 suffers more pressure drop than X-50 while working in the same operating conditions due to small pore size and fiber diameter as compared to X-50 module. Moreover, pressure drop of organic phase is greater than aqueous phase due to its high viscosity. The increase in feed flow rates adversely affects the extraction efficiency by having less contact time for extracting of copper (II) by TFA from aqueous phase.

Finally, it has been concluded that X-40 module offers better results in terms of flux and extraction efficiency compared to X-50.

7 Notations and Symbols

A_i	Membrane surface area (m^2)
C_{ini}^{Cu2+}	Initial concentration of Cu^{2+} in aqueous phase (molm^{-3})
C_i	Concentration of "i" component (molm^{-3})
C_{ini}^{TFA}	Initial concentration of TFA in organic phase (molm^{-3})
d_{int}	Internal diameter of fiber (m)
d_{ext}	External diameter of fiber (m)
d_{pore}	Mean pore diameter (m)
D	Diffusion coefficient (m^{2}s^{-1})
D_{org}	Diffusion coefficient of copper complex in organic phase (m^2.s^{-1})
Gz	Graetz number
HTU	Height of Transfer Unit
J_i	Flux of "i" component (molm^{-2}min^{-1})
K_{mb}	Membrane side mass transfer coefficient (ms^{-1})
K_i	Mass transfer coefficient of i component (ms^{-1})
NTU	Number of Transfer Unit
P	Partition coefficient
ΔP_c	Critical pressure drop/breakthrough pressure (kPa, psi)
Q_{org}	Volumetric flow rate of organic phase (m^{3}s^{-1})
Q_{aq}	Volumetric flow rate of organic phase (m^3.s^{-1})

R_e	Reynolds number (-)
S_c	Schmidt number (-)
S_h	Sherwood number (-)
Z/L	Module length (m)
σ	Membrane thickness (m)
τ	Tortuosity
θ	Contact angle
ε	Porosity
γ_{aq}	Aqueous phase interfacial tension
γ_{org}	Organic phase interfacial tension
φ_{max}	Maximum extraction efficiency

References

[1] Jadhav, U. U., Hocheng, H. "A review of recovery of metals from industrial waste." *Journal of Achievement in Materials and Manufacuring Engineering*. 54(2), pp. 159-167. 2012.

[2] Zhang, Z. E., Yan Y. F., Zhang, L., Ju, S. X. "Hollow fiber membrane contactor absorption of CO_2 from the flue gas: review and perspective." *Global NEST Journal*. 16(2), pp. 354-373. 2014.

[3] Naim R., Ismail, A. F., Mansourizadeh, A. "Preparation of microporous PVDF hollow fiber membrane contactors for CO_2 stripping from diethanolamine solution." *Journal of Membrane Science.* 392-393, pp. 29-37. 2012. https://doi.org/10.1016/j.memsci.2011.11.040

[4] Gabelman, A., Hwang, S. T. "Hollow fiber membrane contactors." *Journal of Membrane Science.* 159, pp. 61-106. 1999. https://doi.org/10.1016/S0376-7388(99)00040-X

[5] Younas, M., Bocquet, S. D., Sanchez, J. "Kinetic and dynamic study of liquid-liquid extraction of copper in a HFMC: experimentation, modeling, and simulation." *AIChE Journal.* 56(6), pp. 1469-1480. 2010. https://doi.org/10.1002/aic.12076

[6] Lin, S. H., Juang, R. S. "Removal of free and chelated Cu (II) ions from water by a non-dispersive solvent extraction process." *Water Research*. 36(14), pp. 3611-3619. 2002. https://doi.org/10.1016/S0043-1354(02)00074-X

[7] Gonzalez-Munoz, M. J., Luque, S., Alvarez, J. R., Coca, J. "Recovery of phenol from aqueous solutions using hollow fiber contactor." *Journal of Membrane Science*. 213(1-2), pp. 181-193. 2003. https://doi.org/10.1016/S0376-7388(02)00526-4

[8] Juang, R. S., Huang, H. L. "Mechanistic analysis of solvent extraction of heavy metals in membrane contactors." *Journal of Membrane Science*. 213(1-2), pp. 125-135. 2003. https://doi.org/10.1016/S0376-7388(02)00519-7

[9] Bocquet, S. D., Torres, A., Sanchez, J., Rios, M. "Modeling the mass transfer in solvent-extraction processes with hollow-fiber membranes." *AIChE Journal*. 51(4), pp. 1067-1079. 2005. https://doi.org/10.1002/aic.10461

[10] Niessner, J., Hassanizadeh, S. M. " Mass and Heat Transfer During Two-Phase Flow in Porous Media - Theory and Modeling." In: El-Amin, M. (ed.) *Mass transfer in multiphase systems and its applications*. InTech Publishers. 2011. https://doi.org/10.5772/14299

[11] Boributha, S., Rongwonga, W., Assabumrungrat, S., Laosiripojana, N., Jiraratananon, R. "Mathematical modeling and cascade design of hollow fiber membrane contactor for CO2 absorption by monoethanolamine." *Journal of Membrane Science*. 401-402, pp. 175-189. 2012. https://doi.org/10.1016/j.memsci.2012.01.048

[12] Treybal, R. E. "*Mass-transfer operations*." McGraw Hill book co. Singapore, 1981.

[13] Nagy, E., Dudás, J., Mazzei, R., Drioli, E., Giorno, L. "Description of the diffusive–convective mass transport in a hollow-fiber biphasic biocatalytic membrane reactor." *Journal of Membrane Science*. 482, pp. 144-157. 2015. https://doi.org/10.1016/j.memsci.2014.11.060

[14] Pierre, F. X., Souchon, I., Marin, M. "Recovery of sulphur aroma compounds using membrane based solvent extraction." *Journal of Membrane Science*. 187(1-2), pp. 239-253. 2001. https://doi.org/10.1016/S0376-7388(01)00352-0

[15] Wickramasinghe, S. R., Semmens, M. J., Cussler, E. L. "Mass transfer in various hollow fiber geometries." *Journal of Membrane Science*. 69(3), pp. 235-250. 1992. https://doi.org/10.1016/0376-7388(92)80042-I

[16] Lipnizki, F., Field, R. W. "Mass transfer performance for hollow fiber modules with shell-side axial feed flow: using an engineering approach to develop a framework." *Journal of Membrane Science*. 193(2), pp. 195-208. 2001. https://doi.org/10.1016/S0376-7388(01)00512-9

[17] Prasad, R., Sirkar, K. K. "Dispersion-free solvent extraction with microporous hollow-fiber modules." *AIChE Journal*. 34, pp. 177-188. 1988. https://doi.org/10.1002/aic.690340202

[18] Viegas, R. M. C., Rodriguez, M., Luque, S., Alvarez, J. R., Coelhoso, I. M., Crespo, J. P. S. G. "Mass transfer correlations in membrane extraction: Analysis of Wilson-plot Methodology." *Journal of Membrane Science*. 145(1), pp. 129-142. 1998. https://doi.org/10.1016/S0376-7388(98)00074-X

[19] Kiani, A., Bhave, R. R., Sirkar, K. K. "Solvent extraction with immobilized interfaces in a microporous hydrophobic membrane." *Journal of Membrane Science.* 20, pp. 125-140. 1984. https://doi.org/10.1016/S0376-7388(00)81328-9

[20] Iversen, S. B., Bhatia, V. K., Dam-Johansen, K., Jonsson, G. "Characterization of micro-porous membranes for use in membrane contactors." *Journal of Membrane Science*. 130(1-2), pp. 205-217. 1997. https://doi.org/10.1016/S0376-7388(97)00026-4

[21] Kumar, A., Haddad, R., Alguacil, F. J., Sastre, A. M. "Comparative performance of non-dispersive solvent extraction using a single module and the integrated membrane Process with two hollow fiber contactors." *Journal of Membrane Science*. 248(1-2), pp. 1-14. 2005. https://doi.org/10.1016/j.memsci.2004.09.003

[22] Souchon, I., Athes, V., Pierre, F. X., Marin, M. "Liquid–liquid extraction and air stripping in membrane contactor: application to aroma compounds recovery." *Desalination*. 163(1-3), pp. 39-46. 2004. https://doi.org/10.1016/S0011-9164(04)90174-9

[23] Yang, C., Cussler, E. L. "Reactive extraction of penicillin G in hollow fiber and hollow fiber fabric modules." *Biotechnology and Bioengineering*. 69(1), pp. 66-73. 2000. https://doi.org/10.1002/(SICI)10970290(20000705)69:1<66::AID-BIT8>3.0.CO;2-I

[24] Viladomat, F. G., Souchon, I., Pierre, F. X., Marin, M. "Liquid-liquid and liquid-gas extraction of aroma compounds with hollow fibers." *AIChE Journal*. 52(6), pp. 2079-2088. 2006. https://doi.org/10.1002/aic.10827

[25] Fouad, E. A., Bart, H. J. "Emulsion liquid membrane extraction of zinc by a hollow-fiber contactor." *Journal of Membrane Science*. 307(2), pp. 156-168. 2008. https://doi.org/10.1016/j.memsci.2007.09.043

[26] Sciubba, L., Di-Gioia, D., Fava, F., Gostoli, C. "Membrane-based solvent extraction of vanillin in hollow fiber contactors." *Desalination*. 241(1-3), pp. 357-364. 2009. https://doi.org/10.1016/j.desal.2007.10.104

[27] Younas, M., Boucquet, S. D., Sanchez, J. "Experimental and theoretical mass transfer transient analysis of copper extraction using hollow fiber membrane contactors." *Journal of Membrane Science*. 382(1-2), pp. 70-81. 2011. https://doi.org/10.1016/j.memsci.2011.07.040

[28] Roudet, M., Loubiere, K., Gourdon, C., Cabassud, M. "Hydrodynamic and mass transfer in inertial gas–liquid flow regimes through straight and meandering millimetric square channels." *Chemical Engineering Science*. 66(13), pp. 2974-2990. 2011. https://doi.org/10.1016/j.ces.2011.03.045

[29] Russell, T. W. F., Robinson, A. S., Wagner, N. J. "*Mass and heat transfer: analysis of mass contactors and heat exchangers*." Cambridge University Press, New York. 2008.

[30] Treybal, R. E. "*Mass Transfer Operations*." 3rd ed., McGraw-Hill, New York, 1980.

[31] Zheng, J., Dai, Z. W., Wong, F., Xu, Z. K. "Shell side mass transfer in a transverse flow hollow fiber membrane contactor." *Journal of Membrane Science*. 261(1-2), pp. 114-120. 2005. https://doi.org/10.1016/j.memsci.2005.02.035

[32] Prasad, R., Sirkar, K. K. "Hollow fiber solvent extraction: performances and design." *Journal of Membrane Science*. 50(2), pp. 153-175. 1990. https://doi.org/10.1016/S0376-7388(00)80313-0

[33] Costello, M. J., Fane, A. G., Hogan, P. A., Schofield, R. W. "The effect of shell side hydrodynamics on the performance of axial flow hollow fibre modules." *Journal of Membrane Science*. 80(1), pp. 1-11. 1993. https://doi.org/10.1016/0376-7388(93)85127-I

[34] Cussler, E. L. "Hollow fiber contactors." In: Crespo, J. G., Bo Èddeker, K. W. (eds.) *Membrane processes in separation and purification*. Kluwer Academic Publishers, Netherlands, pp. 375-394. 1994.

[35] Zhang, W., Hao, Z., Chen, G., Li, J., Li, Z., Wang, Z., Ren, Z. "Effect of porosity on mass transfer of gas absorption in a hollow fiber membrane contactor." *Journal of Membrane Science*. 470(15), pp. 399-410. 2014. https://doi.org/10.1016/j.memsci.2014.06.059